Наносистеми, наноматеріали, нанотехнології
Nanosistemi, Nanomateriali, Nanotehnologii
2023, т. 21, № 4, сс. 709–720

PACS numbers: 61.72.Mm, 68.35.Ct, 68.37.Ps, 68.55.A-, 68.55.J-, 81.15.Cd, 82.80.Pv

Surface Morphology of $ZnGa_2O_4$:Cr Thin Films Obtained by RF Ion-Plasma Sputtering

O. M. Bordun[1], I. O. Bordun[1], I. I. Medvid[1], M. V. Protsak[1], I. Yo. Kukharskyy[1], V. G. Bihday[1], I. M. Kofliuk[1], I. Yu. Khomyshyn[1], and D. S. Leonov[2]

[1]*Ivan Franko National University of Lviv, 50, Drahomanov Str., UA-79005 Lviv, Ukraine*
[2]*Technical Centre, N.A.S. of Ukraine, 13, Pokrovska Str., UA-04070 Kyiv, Ukraine*

Thin $ZnGa_2O_4$:Cr films are obtained by radio-frequency (RF) ion-plasma sputtering in an argon atmosphere on the single-crystal NaCl and amorphous υ-SiO_2 substrates. The study of the surface morphology of thin films by atomic force microscopy (AFM) shows that the average diameter of the grains forming the film surface decreases from 320 nm to 211 nm, when switching over from NaCl substrates to υ-SiO_2 ones. The heat treatment of films on υ-SiO_2 substrates in an argon atmosphere has weak effect on the average grain diameter, while heat treatment in an air leads to an increase in the average grain diameter to 316 nm. XPS spectra show that, after high-temperature annealing, the studied films may contain an excessive presence of the Ga_2O_3 phase in addition to the $ZnGa_2O_4$ phase. It has been found that, when $ZnGa_2O_4$:Cr films are annealed in an air, grain growth occurs along the film surface, and when annealed in an argon atmosphere, grain growth occurs perpendicularly to the film surface.

Методом високочастотного (ВЧ) йонно-плазмового розпорошення в атмосфері арґону на монокристалічних підкладинках NaCl та аморфних підкладинках υ-SiO_2 одержано тонкі плівки $ZnGa_2O_4$:Cr. Дослідження морфології поверхні тонких плівок методом атомно-силової мікроскопії (АСМ) показали, що з переходом від підкладинок NaCl до υ-SiO_2 середній діяметер зерен, що формують поверхню плівки, зменшується від 320 нм до 211 нм. Термооброблення плівок на підкладинках з υ-SiO_2 в атмосфері арґону слабо впливає на середній діяметер зерен, а термооброблення на повітрі приводить до зростання середнього діяметра зерен до 316 нм. На основі XPS-спектрів показано, що після високотемпературного відпалу у досліджуваних плівках, окрім фази $ZnGa_2O_4$, можли-

ва надлишкова присутність фази Ga_2O_3. Встановлено, що за відпалу плівок $ZnGa_2O_4$:Cr на повітрі відбувається зростання зерен вздовж поверхні плівки, а за відпалу в атмосфері арґону відбувається зростання зерен перпендикулярно до поверхні плівки.

Key words: zinc gallate, chrome activator, thin films, crystallites, surface morphology.

Ключові слова: ґалат Цинку, хромистий активатор, тонкі плівки, кристаліти, морфологія поверхні.

(Received 6 November, 2023)

1. INTRODUCTION

Recently, due to the widespread use of metal oxide thin films in optoelectronics and instrumentation [1–6], researchers have shown interest in studying the properties of zinc gallate-based thin films— $ZnGa_2O_4$. Due to their good optical, dielectric, and performance properties, pure and activated $ZnGa_2O_4$ thin films are widely used in vacuum fluorescent and field emission displays, electronic devices, and gas sensors [7–16]. A wide range of studies on one-dimensional zinc gallate $ZnGa_2O_4$ nanostructures (nanoparticles, nanowires, and nanotubes) has shown that such one-dimensional nanostructures are characterized by quite interesting optical and electrical properties [17–21]. However, researchers have questions about the reliability and stability of such nanostructures. The problems mentioned earlier can be overcome by using nanometre thin film structures. At the same time, both pure and activated $ZnGa_2O_4$ films exhibit effective luminescent properties and are widely studied for practical use in electron-optical devices [22–24]. Based on this, an important task arises to develop and improve thin-film materials based on $ZnGa_2O_4$ to expand the potential scope of their use. In general, the question of the physical properties of thin films is complicated by the fact that films do not always have a perfect structure. Obtaining the required and stable reproducible properties of polycrystalline films is further complicated by the presence of intergranular boundaries (IGBs). The physical properties of polycrystalline thin films are largely determined not only by the material properties but also by the energy levels arising from the presence of the IMBs. It is clear that such levels are also determined by the size of the crystallites that form the thin films. This leads to the study of the surface morphology of $ZnGa_2O_4$ thin films using atomic force microscopy (AFM). The films in this work were obtained by the method of RF ion-plasma sputtering, which is optimal for obtaining homogeneous semiconductor and dielectric films [25].

2. EXPERIMENTAL TECHNIQUE

Thin $ZnGa_2O_4$:Cr films with a thickness of 0.3–1.0 μm were obtained by RF ion plasma sputtering on single-crystal NaCl substrates and amorphous fused quartz υ-SiO_2 substrates. The RF sputtering was carried out in an argon atmosphere in a system using the magnetic field of external solenoids for compression and additional ionization of the plasma column. The feedstock was a mixture of ZnO and Ga_2O_3 oxides of the 'ОСЧ' grade (extra pure) of stoichiometric composition. The concentration of Cr^{3+} activator was of 1 mol.%. After the films were deposited on υ-SiO_2 substrates, they were heat treated in argon and air at 1000–1100°C.

The structure and phase composition of the obtained films were studied by x-ray diffraction analysis (Shimadzu XDR-600). X-ray diffraction studies have shown the presence of a polycrystalline structure with a predominant orientation in the (022), (113), (004), and (333) planes. The characteristic diffractograms of $ZnGa_2O_4$ thin films were presented earlier in our work [26].

Using an OXFORD INCA Energy 350 energy dispersive spectrometer, elemental analysis of the samples was performed at several points on the surface of the films. The calculations confirmed that the percentage of components in the obtained films corresponded to their percentage in the $ZnGa_2O_4$:Cr compound.

The elemental composition of the surface of the obtained thin films was analysed by x-ray photoelectron spectroscopy (XPS). The XPS spectra (XPS, Phoibos 150, Specs) were recorded using a monochromatic x-ray source AlK_α (1486.6 eV) and a hemispherical SPECS analyser, HSA 3500. The binding energy was calibrated against the signal from C1*s* at 285.0 eV.

The surface morphology of the films was studied using an INTEGRA TS-150 atomic force microscope (AFM).

3. RESULTS AND DISCUSSION

Microphotographs of the surface of $ZnGa_2O_4$:Cr films obtained by RF ion plasma sputtering on NaCl and υ-SiO_2 substrates without heat treatment are shown in Fig. 1 and, after heat treatment in the atmosphere of air and argon, are shown in Fig. 2.

The topography of the samples was quantitatively characterized by standard parameters: root mean square roughness, maximum grain height, average grain diameter, average grain area, and grain volume, which were calculated from AFM data for areas of the same size (5000×5000 nm).

The characteristic parameters of $ZnGa_2O_4$:Cr thin films on various substrates without heat treatment and after heat treatment in

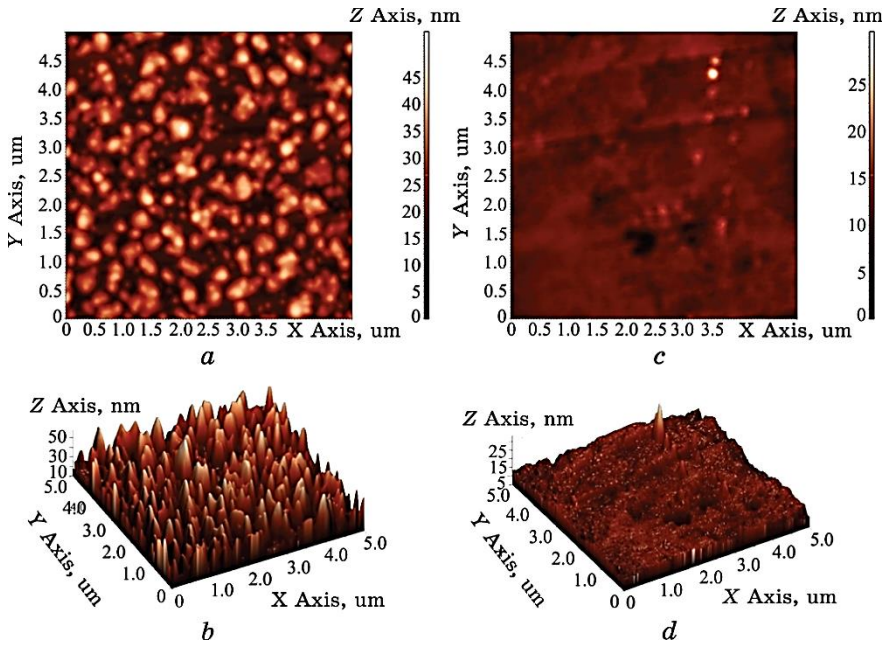

Fig. 1. Images of the surface morphology of $ZnGa_2O_4$:Cr thin films obtained by RF sputtering without heat treatment on υ-SiO_2 (*a*, *b*) and NaCl (*c*, *d*) substrates. Images *a* and *c* are two-dimensional, *b* and *d* are three-dimensional.

the atmosphere of air and argon are given in Table.

As can be seen from the results obtained, the change in the type of substrate and the presence of heat treatment has a significant impact on the size of crystal grains and surface roughness of the films.

The analysis of AFM images (Fig. 1 and Fig. 2) and crystal grain parameters (Table) of the surface of $ZnGa_2O_4$:Cr films shows that films deposited on amorphous quartz υ-SiO_2 substrate are formed from larger grains than when sputtered on a single-crystal NaCl substrate. The size of crystallites of $ZnGa_2O_4$:Cr thin films sputtered on the υ-SiO_2 substrate after heat treatment in the atmosphere of air and argon increased significantly. Such an increase in the size of crystalline grains and, in particular, an increase in the average grain diameter and changes in the value of the root mean square roughness indicate a complication of the surface structure.

A comparison of the histograms of the grain height distribution (Fig. 3) shows that, on NaCl substrates, lower grains are formed, from which the surface of $ZnGa_2O_4$:Cr thin films is formed. At the same time, their diameters are significantly larger (≅ 1.5 times)

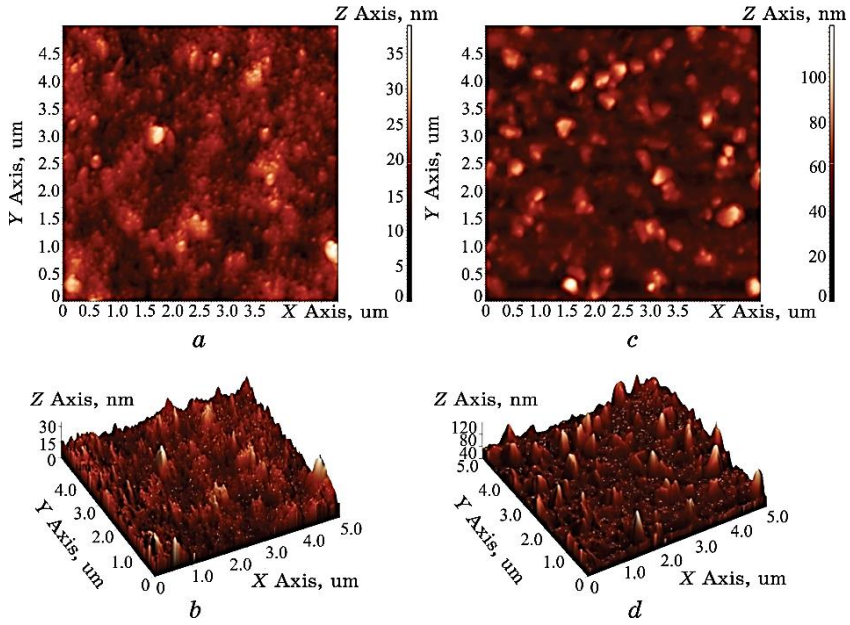

Fig. 2. Images of the surface morphology of $ZnGa_2O_4$:Cr thin films obtained by RF sputtering on υ-SiO_2 substrates after heat treatment in air (*a*, *b*) and argon (*c*, *d*). Images *a* and *c* are two-dimensional, *b* and *d* are three-dimensional.

than those of the unannealed films sputtered on a quartz substrate. The heat treatment of $ZnGa_2O_4$:Cr thin films in an argon atmosphere significantly affects the increase in grain height compared to unannealed films and films annealed in an air atmosphere. In particular, if we compare the RMS surface roughness of thin films, it is the lowest for films deposited on NaCl substrates compared to unannealed films and films subjected to heat treatment in the air and argon atmosphere deposited on quartz substrates. The annealing of films in an argon atmosphere leads to an increase in this parameter (by $\cong 1.5$ times) compared to unannealed films. For the films annealed in the air atmosphere, a decrease in the value of this parameter is observed compared to the unannealed $ZnGa_2O_4$:Cr films ($\cong 2.2$ times).

The increase in the size of crystalline grains and the simultaneous decrease in the concentration of grains in $ZnGa_2O_4$:Cr thin films after heat treatment (Table) indicates the possibility of the transition of the film surface to a more nanostructured state due to the crystallization of the surface layer.

In addition, it can be assumed that the change in the surface morphology of $ZnGa_2O_4$:Cr thin films after annealing in air and ar-

TABLE. Parameters of crystal grains of $ZnGa_2O_4$:Cr thin films.

Parameters	Without heat treatment on the substrate NaCl	Without heat treatment on the substrate υ-SiO_2	Heat treatment in air on the substrate υ-SiO_2	Heat treatment in Ar on the substrate υ-SiO_2
Average grain diameter, nm	320	211	316	222
Average square roughness, nm	1.7	9,6	4.4	14.6
Maximum grain height, nm	9.6	11	12	28
Average grain area, nm^2	32200	12100	30400	16100
Average grain volume, nm^3	35900	67600	115000	121000

gon (Fig. 2) is to some extent related to the fact that Zn atoms diffuse from the film at high annealing temperatures. After annealing the films at high temperatures, in addition to the $ZnGa_2O_4$ phase, the presence of the Ga_2O_3 phase is possible, as observed in Ref. [27].

Some excess of Ga_2O_3 in the structure of $ZnGa_2O_4$:Cr spinel is confirmed by luminescence studies conducted in [28, 29].

This is also confirmed by our XPS spectra for unannealed $ZnGa_2O_4$:Cr thin films and annealed films in the air (Fig. 4). In particular, it was found that for the annealed film, a less intense peak corresponding to the Zn (2*p*) atom was observed in the spectrum compared to the unannealed film. In addition, the intensity of the peaks corresponding to Ga (3*p*) and O (1*s*) atoms for the annealed films is significantly higher compared to the unannealed films.

The characteristic distributions of grain diameter sizes in $ZnGa_2O_4$:Cr thin films depending on the type of substrate and the presence of heat treatment are shown in Fig. 5.

A thorough review [30] analysed the growth of crystal grains in thin films and the evolution of crystal structures and showed that polycrystalline thin films with thicknesses up to 1 μm, which is typical for our $ZnGa_2O_4$:Cr films, often have 2*D*-like structures. In such structures, most grain boundaries are perpendicular to the film surface. Most of the materials analysed in [30] form films of nonequilibrium grains with dimensions smaller than the film thickness and form two-dimensional structures only after annealing. Based on numerical results, authors of [30] also concluded that grain formation in thin films is difficult to describe accurately us-

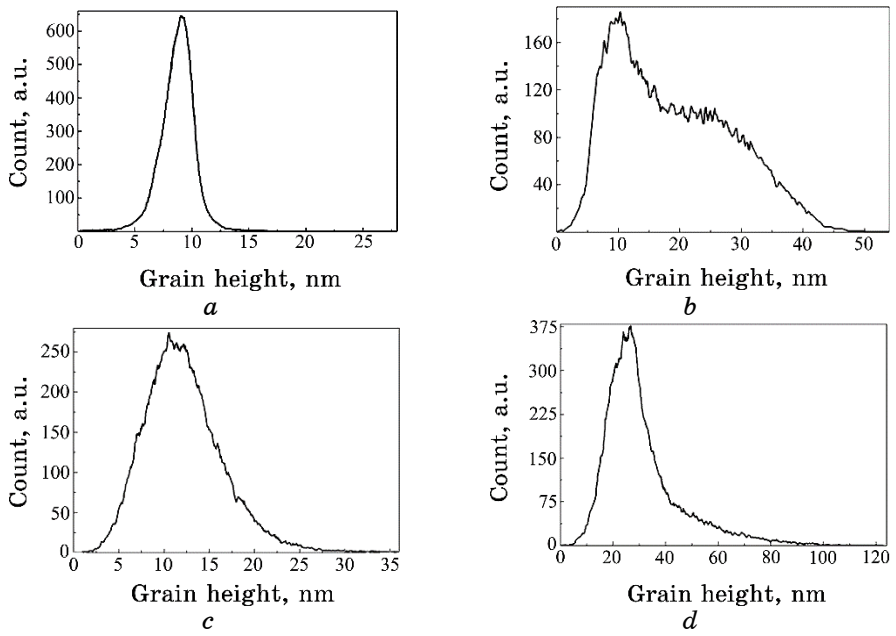

Fig. 3. Grain height distribution on AFM images of $ZnGa_2O_4$:Cr thin films obtained by RF sputtering without heat treatment on NaCl (*a*), υ-SiO_2 (*b*) substrates and after heat treatment in air (*c*) and argon (*d*) on υ-SiO_2 substrates.

ing modelling or comparison with experiments that describe the study of foams or monolayers. In general, grain sizes in polycrystalline films are lognormally distributed in size.

In some cases, further grain growth is observed due to 'anomalous' growth or preferential growth of several grains, which usually have specific crystallographic orientation relations relative to the surface plane of the substrate. Our results show that this situation is most likely to be typical for the $ZnGa_2O_4$:Cr films, which we have obtained. When the number of growing grains leads to a 'matrix' of grains beyond the static boundaries, a bimodal grain size distribution develops, which is called secondary grain growth [31]. Grains growing abnormally often have a limited or homogeneous texture. Secondary grain growth in thin films typically involves an evolution in the grain texture distribution as well as an evolution in the grain size distribution.

Our results of the distribution of grain diameter sizes in $ZnGa_2O_4$:Cr thin films (Fig. 5) indicate that, when these films are deposited on NaCl substrates, a bimodal distribution of diameters with a maximum in the 320 nm region is observed. On the growing

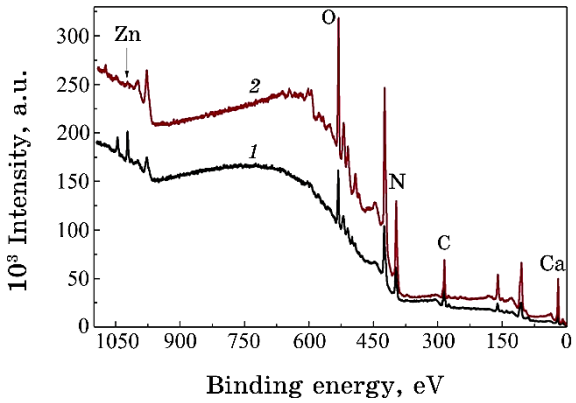

Fig. 4. XPS spectra of the surface of unannealed (*1*) and air-annealed (*2*) $ZnGa_2O_4$:Cr thin films.

part of the distribution, a small local maximum appears in the 220 nm region that indicates the presence of nonequilibrium grain growth. A more complex shape of the diameter distribution is formed, when films are deposited on an amorphous υ-SiO_2 substrate. In particular, for freshly deposited films (Fig. 5, *b*), a trimodal distribution with maxima in the region of 100, 145, and 220 nm is clearly visible. After heat treatment of such films in air, a unimodal distribution is observed (Fig. 5, *c*) with a maximum in the 280nm region. Sometimes, such cases occur, when grains are distributed by diameter in polycrystalline films [32]. In particular, this situation is observed during the RF deposition of Y_2O_3:Eu thin films [33]. After heat treatment of the films in argon (Fig. 5, *d*), a trimodal distribution with maxima in the regions of 200 and 260 nm, as well as a local maximum in the region of 140 nm, are observed.

Summarising the situation described above, it can be concluded that the growth of secondary and tertiary grains occurs during the heat treatment process. It should be noted that a similar situation is observed during RF deposition on υ-SiO_2 substrates and β-Ga_2O_3 thin films [34]. The growth of secondary and tertiary grains was observed in these films during both the RF sputtering and heat treatment processes.

Taking into account the presence of 'anomalous' grain growth and grain growth with specific crystallographic orientation relations relative to the substrate surface plane, we consider the features of grain volumes in $ZnGa_2O_4$:Cr thin films.

Based on Fig. 1 and Fig. 2, as well as the data in Table 1, it can be seen that, after depositing thin $ZnGa_2O_4$:Cr films on amorphous υ-SiO_2 substrates, the heat treatment results in the growth of crystalline grains that form the film. At the same time, annealing in air

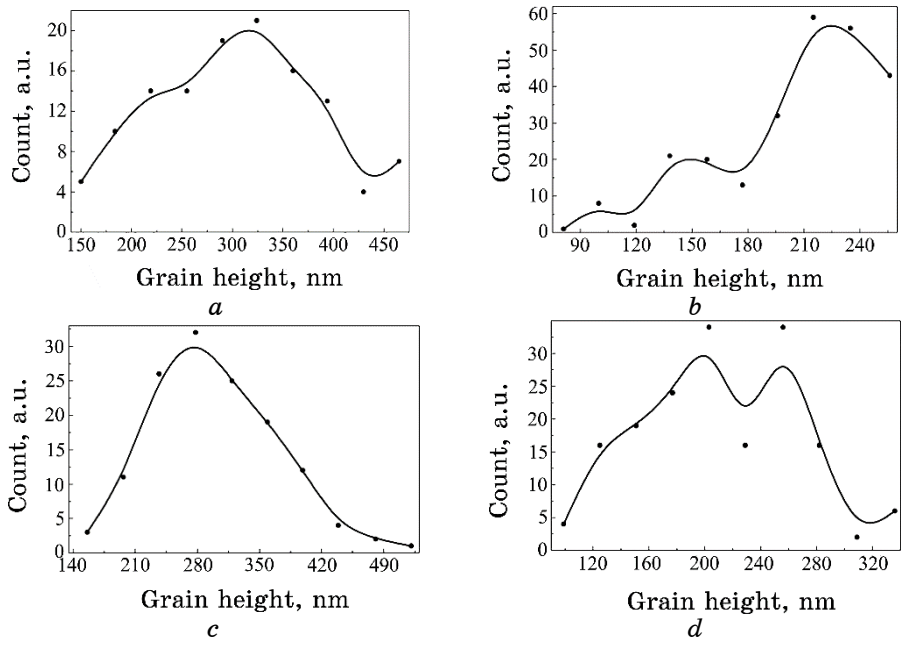

Fig. 5. Distribution of grain diameter sizes and calculated approximated diameter distribution on AFM images of $ZnGa_2O_4$:Cr thin films without heat treatment on NaCl (*a*), υ-SiO_2 (*b*) substrates and after heat treatment in air (*c*) and in argon (*d*) on υ-SiO_2 substrates.

is accompanied by a significant increase in the average grain diameter (≅ 1.5 times) with a significant decrease in the root mean square roughness (≅ 2 times). During annealing in an argon atmosphere, a rather insignificant increase in the average grain diameter and a significant increase in the root mean square surface roughness (≅ 1.5 times) are observed. It is characteristic that both values of the average grain volume are practically quite close and almost 2 times higher than the grain volume in the unannealed films.

The obtained results show that, during the annealing of freshly deposited $ZnGa_2O_4$:Cr films in air, grain growth occurs along the film surface. At the same time, the annealing of these films in an argon atmosphere is accompanied by grain growth perpendicularly to the film surface.

4. CONCLUSIONS

It has been established that thin films of $ZnGa_2O_4$:Cr spinel formed from nanometre grains are formed by RF ion-plasma sputtering on single-crystal NaCl and amorphous υ-SiO_2 substrates. Based on the

AFM images, it is shown that the average diameters of the crystallites of the films on NaCl substrates are of 320 nm, and on υ-SiO_2 substrates, they are of 211 nm. The heat treatment of films on υ-SiO_2 substrates in air leads to an increase in the average grain diameters to 316 nm and, accordingly, the root mean square roughness from 9.6 to 4.4 nm. Heat treatment of such films in an argon atmosphere leads to an increase in the average grain diameter to 222 nm and the root mean square surface roughness to 14.6 nm. Based on the analysis of the results of the distribution of grain diameter sizes, it is proposed that secondary and tertiary grains grow during the RF sputtering process and during heat treatment. It has been shown that, after annealing at high temperatures, in addition to the $ZnGa_2O_4$ phase, the Ga_2O_3 phase may be present in the studied films. It was found that, when $ZnGa_2O_4$:Cr films are annealed in air, grain growth occurs along the film surface, and when annealed in an argon atmosphere, grain growth occurs perpendicularly to the film surface.

REFERENCES

1. X. Yu, T. Marks and A. Facchetti, *Nature Mater.*, **15**: 383 (2016); https://doi.org/10.1038/nmat4599
2. P. Koralli, S. F. Varol, G. Mousdis, D. E. Mouzakis, Z. Merdan, and M. Kompitsas, *Chemosensors*, **10**: 162 (2022); https://doi.org/10.3390/chemosensors10050162
3. O. M. Bordun and A. T. Stets'kiv, *J. Appl. Spectrosc.*, **68**, No. 5: 882 (2001); https://doi.org/10.1023/A:1013266505668
4. A. Das and D. Basak, *ACS Appl. Electron. Mater.*, **3**, No. 9: 3693 (2021); https://doi.org/10.1021/acsaelm.1c00393
5. O. M. Bordun, B. O. Bordun, I. M. Kofliuk, I. Yo. Kukharskyy, I. I. Medvid, and M. V. Protsak, *IEEE XIIth International Conference on Electronics and Information Technologies (ELIT) (19–21, May 2021, Lviv, Ukraine)*, p. 33–36; https://doi.org/10.1109/ELIT53502.2021.9501095
6. P. Sakthivel, R. Murugan, S. Asaithambi, M. Karuppaiah, S. Rajendran, and G. Ravi, *J. Phys. Chem. of Solids*, **126**: 1 (2019); https://doi.org/10.1016/j.jpcs.2018.10.031
7. R.-H. Horng, Ch.-Yi Huang, S.-L. Ou, T.-K. Juang, and P.-L. Liu, *Cryst. Growth Des.*, **17**, No. 11: 6071 (2017); https://doi.org/10.1021/acs.cgd.7b01159
8. Ch.-Ch. Yen, A. K. Singh, H. Chang, K.-P. Chang, P.-W. Chen, P.-L. Liu, and D.-S. Wuu, *Appl. Surf. Science*, **597**: 153700 (2022); https://doi.org/10.1016/j.apsusc.2022.153700
9. H. Lee, Ch. W. Bark, and H. W. Cho, *Jpn. J. Appl. Phys.*, **58**: SDDE15 (2019); https://doi.org/10.7567/1347-4065/ab1478
10. Zh. Jiao, G. Ye, F. Chen, M. Li, and J. Liu, *Sensors*, **2**: 71 (2002); https://doi.org/10.3390/s20300071
11. Y. E. Lee, D. P. Norton, J. D. Budai, and Y. Wei, *J. Appl. Phys.*, **90**, No. 8:

3863 (2001); https://doi.org/10.1063/1.1396829
12. S.-H. Tsai, Yu.-Ch. Shen, Ch.-Yi Huang, and R.-H. Horng, *Appl. Surf. Science*, **496**: 143670 (2019); https://doi.org/10.1016/j.apsusc.2019.143670
13. M. N. da Silva, J. M. de Carvalho, M. C. de Abreu Fantini, L. A. Chiavacci, and C. Bourgaux, *ACS Appl. Nano Mater.*, **2**, No. 11: 6918 (2019); https://doi.org/10.1016/j.cofs.2019.08.010
14. A. Guo, L. Zhang, N. Cao, T. Lu, Y. Zhu, D. Tian, Zh. Zhou, Sh. He, B. Xia, and F. Zhao, *Appl. Phys. Express*, **16**: 021004 (2023); https://doi.org/10.35848/1882-0786/acb98c
15. Y. Liu, T. Zheng, X. Zhang, and Ch. Chen, *Scientific Reports*, **13**: 14430 (2023); https://doi.org/10.1038/s41598-023-41658-5
16. O. M. Bordun, V. G. Bihday, and I. Yo. Kukharskyy, *J. Appl. Spectrosc.*, **80**, No. 5: 721 (2013); https://doi.org/10.1007/s10812-013-9832-2
17. Ch. S. Kamal, S. Boddu, B. Vishwanadh, K. R. Rao, V. Sudarsan, and R. K. Vatsa, *J. Lumin.*, **188**: 429 (2017); https://doi.org/10.1016/j.jlumin.2017.04.056
18. H. Liang, F. Meng, B. K. Lamb, Q. Ding, L. Li, Zh. Wang, and S. Jin, *Chem. Mater.*, **29**, No. 17: 7278 (2017); https://doi.org/10.1021/acs.chemmater.7b01930
19. M. Hirano, Sh. Okumura, Y. Hasegawa, and M. Inagaki, *Intern. J. Inorg. Mater.*, **3**: 797 (2001); https://doi.org/10.1016/S1466-6049(01)00178-7
20. Z. Lou, L. Li, and G. Shen, *Nano Res.*, **8**: 2162 (2015); https://doi.org/10.1007/s12274-015-0723-0
21. A. Sood, F.-G. Tarntair, Yu-X. Wang, T.-Ch. Chang, Yu-H. Chen, P.-L. Liu, and R.-H. Horng, *Results in Physics*, **29**: 104764 (2021); https://doi.org/10.1016/j.rinp.2021.104764
22. Y. Jang, S. Hong, J. Seo, H. Cho, K. Char, and Z. Galazka, *Appl. Phys. Lett.*, **116**: 202104 (2020); https://doi.org/10.1063/5.0007716
23. P. D. Rack, J. J. Peterson, M. D. Potter, and W. Park, *J. Mater. Res.*, **16**, No. 5: 1429 (2001); https://doi.org/10.1557/JMR.2001.0199
24. P. Dhak, U. K. Gayen, S. Mishra, P. Pramanik, and A. Roy, *J. Appl. Phys.*, **106**, No. 6: 063721 (2009); https://doi.org/10.1063/1.3224866
25. K. Wasa, M. Kitabatake, and H. Adachi, *Thin Film Materials Technology: Sputtering of Compound Materials* (Springer-Verlag GmbH&Co. KG–William Andrew Inc. Publishing: 2004).
26. O. M. Bordun, I. Yo. Kukharskyy, and V. G. Bihday, *J. Appl. Spectrosc.*, **78**, No. 6: 922 (2012); https://doi.org/10.1007/s10812-012-9555-9
27. W.-K. Wang, K.-F. Liu, P.-Ch. Tsai, Y.-J. Xu, and Sh.-Y. Huang, *Coatings*, **9**, No. 12: 859 (2019); https://doi.org/10.3390/coatings9120859
28. O. M. Bordun, V. G. Bihday, and I. Yo. Kukharskyy, *J. Appl. Spectrosc.*, **81**, No. 1: 43 (2014); https://doi.org/10.1007/s10812-014-9884-y
29. O. M. Bordun, I. Y. Kukharskyy, and B. O. Bordun, *Physics and Chemistry of Solid State*, **16**, No. 1: 74 (2015) (in Ukrainian); https://doi.org/10.15330/pcss.16.1.74-78
30. C. V. Thompson, *Sol. State Phys.*, **55**: 269 (2001); https://doi.org/10.1016/S0081-1947(01)80006-0
31. C. V. Thompson, *J. Appl. Phys.*, **58**, No. 2: 763 (1985); https://doi.org/10.1063/1.336194
32. C. V. Thompson, *Interface Science*, **6**: 85 (1998);

https://doi.org/10.1023/A:1008616620663
33. O. M. Bordun, I. O. Bordun, I. M. Kofliuk, I. Yo. Kukharskyy, I. I. Medvid, Zh. Ya. Tsapovska, and D. S. Leonov, *Nanosistemi, Nanomateriali, Nanotehnologii*, **20**, Iss. 1: 91 (2022); https://doi.org/10.15407/nnn.20.01.091
34. O. M. Bordun, B. O. Bordun, I. Yo. Kukharskyy, I. I. Medvid, I. I. Polovynko, Zh. Ya. Tsapovska, and D. S. Leonov, *Nanosistemi, Nanomateriali, Nanotehnologii*, **19**, Iss. 1: 159 (2021); https://doi.org/10.15407/nnn.19.01.159